J. Cent. South Univ. (2022) 29: 3077−3087
DOI: https://doi.org/10.1007/s11771-022-5120-8

Springer

Failure behavior and mechanical properties of novel dieless clinched joints with different sheet thickness ratios

QIN Deng-lin(秦登林)[1, 2], CHEN Chao(陈超)[1, 2]*

1. Light Alloy Research Institute, School of Mechanical and Electrical Engineering, Central South University, Changsha 410083, China;
2. State Key Laboratory of High Performance Complex Manufacturing (Central South University), Changsha 410083, China

Abstract: As one of the advanced and efficient means of joining, the clinching process is capable of joining sheets with different materials or different sheet thicknesses. In this article, a novel modified clinching process, i. e., the dieless clinching process, was executed to join AA6061 aluminum alloy with sheet thicknesses of 1.5, 2.0, 2.5 and 3.0 mm according to different sheet stack-ups. The geometrical characteristics, microhardness distribution, failure behavior, static strength, absorbed energy and instantaneous stiffness of the novel dieless joint were gotten and investigated. The results indicated that the sheet thickness ratio has a notable effect on the failure behavior and mechanical properties of the novel dieless clinched joint, and a relatively large sheet thickness ratio can improve the joint performance when joining sheets with different sheet thicknesses.

Key words: joining; clinching process; sheet thickness ratio; failure behavior; mechanical properties

Cite this article as: QIN Deng-lin, CHEN Chao. Failure behavior and mechanical properties of novel dieless clinched joints with different sheet thickness ratios [J]. Journal of Central South University, 2022, 29(9): 3077−3087. DOI: https://doi.org/10.1007/s11771-022-5120-8.

1 Introduction

Due to the increased challenge of environmental pollution and energy shortages, it is an urgent task for automobile manufacturers to produce cars with better fuel efficiency and fewer pollutant emissions by developing lightweight technologies [1−2]. To this end, some lightweight materials represented by aluminum alloy, which has the superiorities of high specific strength, superior anti-corrosion resistance and excellent formability, are gaining increasingly extensive application in the automotive industry [3−6]. Nevertheless, there are some problems associated with these lightweight materials regarding how to join them. For example, it is considerably difficult to achieve a reliable connection between aluminum alloy sheets by some established methods, e. g., resistance spot welding, due to their high thermal conductivity, low melting point as well as dense superficial oxide layer [7−8]. Hence, developing some alternative joining techniques that are suitable for connecting aluminum alloys is desirable.

Recently, some relatively new mechanical

Foundation item: Project(51805416) supported by the National Natural Science Foundation of China; Project(2019QNRC001) supported by the Young Elite Scientists Sponsorship Program by CAST, China; Project(2021JJ20059) supported by the Hunan Provincial Natural Science Foundation for Excellent Young Scholars, China; Project(2019RS1002) supported by the Huxiang High-Level Talent Gathering Project of Hunan Province, China
Received date: 2022-02-25; **Accepted date:** 2022-04-26
Corresponding author: CHEN Chao, PhD, Professor; E-mail: profchenchao@163.com; ORCID: https://orcid.org/0000-0002-9408-1547

joining processes, e.g., mechanical clinching (MC) and self-pierce riveting (SPR) show increasing potential for joining lightweight materials [9−10]. In the MC process, double or multiple layers of sheets can be controlled to deform plastically and generate interlock structure within them. In the SPR process, an additional rivet is driven to pierce through the top sheet (when joining double layers of sheets) or the top and middle sheets (when joining three layers of sheets) and to hook the bottom sheet [11]. Hence, no heat input is required in the two processes, which makes them more energy-efficient and environment-friendly than those thermal joining methods [12]. Furthermore, neither pre-treatment (e.g. preliminary drilling of the sheet in conventional riveting) nor post-processing (e. g. curing of glue in adhesive joining) procedures are necessary for MC or SPR processes, which ensures their production efficiency in industrial applications [13]. During the SPR process, a semi-tubular rivet (sometimes a solid rivet [14]) is indispensable for the connection of sheets. On the one hand, the existence of the auxiliary rivet can enhance the joint strength by bearing load; but on the other hand, it also adds weight to structures or products. In this regard, the clinching process that connects sheets by sole deformation of sheet material shows greater potential for lightweight design of vehicle structure.

Limited by the comparatively low joint strength, the clinching process has only been used in some vehicle structures where the high load-bearing capacity of joints is not required till now [14−15]. Therefore, considerable effort has been exerted to increase joint strength over the past years. In general terms, joint strength is closely related to the interlock structure. ABE et al [16] proposed an ingenious method to enhance the joint strength when joining ultra-high-strength steel sheets. Before the clinching procedure, pre-forming the lower sheet was operated, which can weaken the pressure of the upper sheet suffered in the clinching process and enlarge the interlock of the final joint. In another research conducted by ABE et al [17], a modified lower die with a bottom angle was presented to improve the sheet material flow in the clinching process. By with this method, clinched joint with a larger interlock and thus higher strength can be obtained. The mainstream way to increase the load-bearing capacity of the clinched joints is optimizing the tool parameters [18−20]. WANG et al [21] proposed an automatic optimization procedure of the tools in clinching. In their study, the Bezier curve was utilized to characterize the outline of the clinching tools, which contributes to finding some potential tool shapes. After tool shape optimization, both the axial and shear strengths of the clinched joint were increased by 43% and 30%, respectively. SCHWARZ et al [22] adopted principal component analysis (PCA) to build the meta-modeling between tool geometry parameters and joint geometric characteristic parameters and utilized the generic algorithm to optimize the clinching tools. Recently, some new joining techniques originated from the conventional clinching technology were presented to enhance joint strength. PENG et al [23] introduced a type of modified clinching process, i. e. the two-strokes flattening clinching, in which, an additional flattening operation is exerted on the protrusion of the initial clinched joint to enlarge the interlocking. MUCHA et al [24−25] proposed a clinch-riveting process that employed a deformable rivet to indirectly generate the interlock structure between sheets. This process is somewhat similar to the self-piercing riveting process except that no sheet is pierced. Furthermore, some hybrid joining methods that could combine the clinching process with other joining techniques (e. g. electromagnetically assisted clinching [26], friction stir clinching [27], hot stamping clinching [28], and resistance spot clinching [29]) were also proposed and studied by scholars.

The high bulge on the joint bottom sheet is one of the major disadvantages of clinching, which hinders the extensive use of this process. For instance, it can not be used in structures where aesthetic or functional surfaces are required. For this issue, much research is focused on how to reduce the bulge height of clinched joints [30−32]. Recently, the authors put forward a novel dieless clinching process that can produce joints with smaller bulge height [33]. Figure 1(a) shows the schematic illustration of the novel dieless clinching process. As can be seen, there are only two parts in the tools of this joining process, i.e. the planar anvil and the shouldered punch, which simplifies the tools of the clinching process to the greatest extent. Furthermore, the utilization of the planar anvil

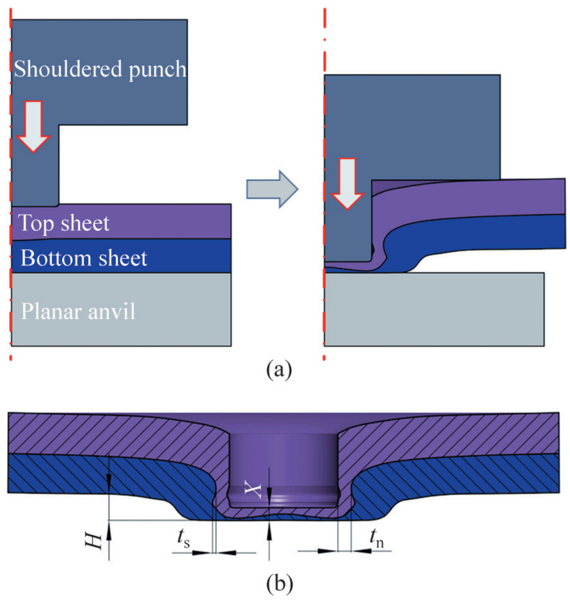

Figure 1 Schematic illustration of the novel dieless clinching process (a) and geometric variables in novel dieless clinched joint (b)

instead of the groove die in the conventional clinching makes it easy for alignment between punch and die, which is essential for the formation of sound joints. There exist mainly four geometric variables (see Figure 1(b)) that can be used to assess the quality of the novel dieless clinched joint, i. e. the neck thickness t_n, the interlock width t_s, the residual sheet thickness X, and the bulge height H. The neck thickness and interlock width are directly related to the joint strength. The residual sheet thickness that reflects the forming degree of sheets in the clinching process can be used for quick detection of joint quality. The residual sheet thickness should not be too small for ensuring the corrosion resistance and water-proof ability of the joint. Besides, the bulge height should be reduced as low as possible in practical application.

One of the main superiorities of the clinching technology is the capacity of joining sheets with different materials or thicknesses [12]. In the last decade, a good deal of research has been performed to study clinching process for joining dissimilar materials, such as steel/aluminium [34], copper/aluminium [35], aluminium/wood [36], aluminium/plastic [37], and aluminum/composite material [38]. However, only a few studies have focused on the clinching technology for joining material with different sheet thicknesses [39−40]. And in-depth research should be carried out to reveal the effect of sheet thickness ratio on the clinching process. To this end, the effect of the sheet thickness ratio (defined as the ratio of top sheet thickness to bottom sheet thickness) on the failure behavior and mechanical properties of the novel dieless clinched joint was experimentally investigated in this study.

2 Experimental procedures

2.1 Experimental materials

AA6061 aluminum alloy, commonly used to manufacture automobile structural parts where bearing load and absorbing energy are required, was utilized as the sheet material for producing the clinched joints in this research [41]. Four types of sheets with diverse thicknesses, i.e 1.5, 2.0, 2.5 and 3.0 mm, were used. All the aluminum plates were cut into strips of 80 mm×20 mm along the rolling direction. Table 1 shows the main mechanical characterization of the AA6061 sheet, which was obtained by the uniaxial tensile tests.

Table 1 Main mechanical characterization of AA6061 sheet

Elastic modulus/ GPa	Yield strength/ MPa	Tensile strength/ MPa	Elongation/ %	Poisson ratio
67.1	302.2	327	9.2%	0.33

2.2 Clinching details

The essential dimension parameters of the dieless clinching tool are shown in Figure 2. This article focuses on the effect of sheet thickness ratio on the novel dieless clinching process. Therefore, a uniform forming force (65 kN) and speed

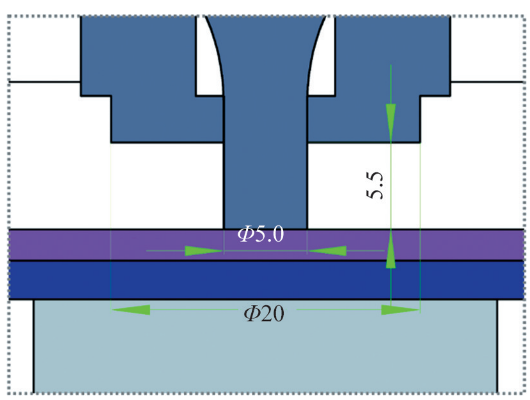

Figure 2 Essential dimension parameters of the dieless clinching tool (unit: mm)

(2 mm/min) were set for all specimens.

The arrangements regarding the sheets with different thicknesses in the clinching process are shown in Table 2. The sheets with the thickness of 1.5, 2.0, 2.5 and 3.0 mm were paired up into four types of sheet stack-ups. For all sheet stack-ups, the total thickness of the sheets stays the same, i. e. 4.5 mm.

Table 2 Paramters of the sheets with different thicknesses in the clinching process

Specimen	Top sheet thickness/mm	Bottom sheet thickness/mm	Sheet thickness ratio
1.5-3	1.5	3.0	0.5
2-2.5	2.0	2.5	0.8
2.5-2	2.5	2.0	1.25
3-1.5	3.0	1.5	2

2.3 Measurement of geometric parameters and microhardness

The joint geometric parameters (shown in Figure 1(b)) are strongly associated with the failure modes and mechanical properties of the clinched joints produced. Hence, the geometric analysis was conducted to reveal the correlation between the joint geometric parameters and joint performance. The joint geometric parameters can be obtained by observing and measuring the joint cross-section. The clinched joints produced were sectioned along their center lines by using a diamond wire cutting machine. Then, a general microscope was utilized to observe the joint cross-section and measure the joint geometric parameters.

In plastic forming processing, the hardness parameters can reflect the degree of material plastic deformation. To make certain the plastic deformation of sheet material in different regions of clinched joint and deeply understand the material flow behavior in the novel dieless clinching process, the microhardness analysis was carried out. After measuring the joint geometric parameters, the cross-sections of joints were mounted in polymeric resin and polished. Then a Buehler 5104 Vickers hardness tester with a 0.05 kg load was used to measure the microhardness distribution within the joint sections.

2.4 Load-bearing capacity tests

To characterize the mechanical properties of the novel dieless clinched joints of various sheet thickness ratios, two load-bearing capacity tests, i.e. tensile-shear test and cross-tension test, were performed by using the aforementioned CMT-5105GJ testing machine. Figure 3 shows the configurations of the clinched joints in the two load-bearing capacity tests. In the tensile-shear test, the specimens were directly fixed on the clamp of the testing machine while in the cross-tension test, a self-designed fixture for the cross joint was used. Spacers were used for the tensile-shear test to ensure that the applied load was along with the joint interface. For each type of joint, three repeated tests were carried out at a consistent test speed of 2 mm/min.

During the load-bearing capacity tests, the testing machine system can automatically record the instantaneous displacement and instantaneous load and plot the load–displacement curves of clinched joints. Figure 4 depicts the schematic illustration of the joint load–displacement curve in load-bearing capacity tests. As can be seen, some important

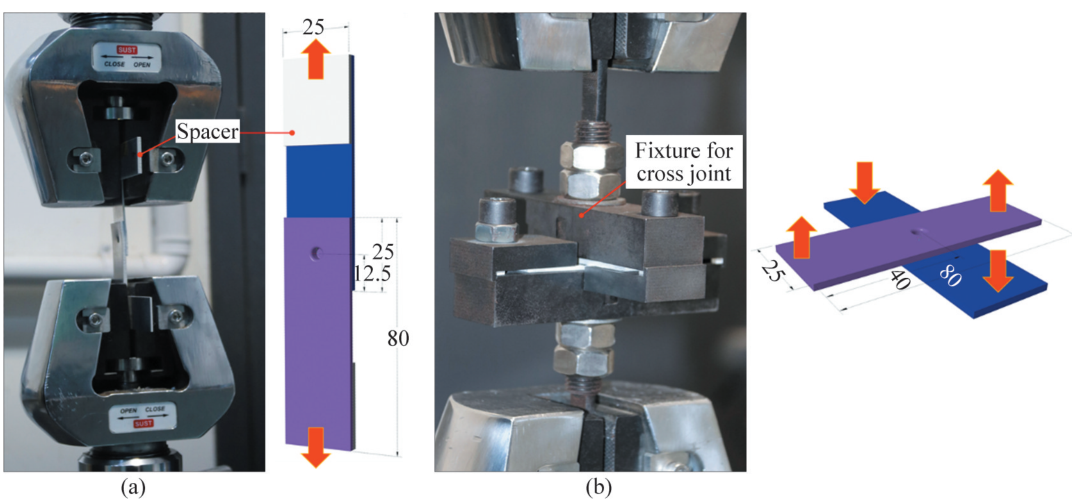

Figure 3 Configurations of the clinched joints in tensile-shear test (a) and cross-tension test (b) (unit: mm)

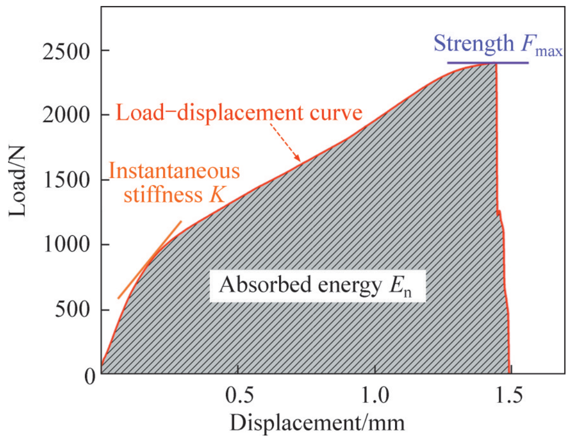

Figure 4 Schematic illustration of the joint load force−displacement curve in load-bearing capacity tests

mechanical characteristics, e. g. the strength F_{max}, instantaneous stiffness K, and absorbed energy E_n can be reflected by the load−displacement curve.

3 Results and discussion

3.1 Geometric and microhardness analysis

Figure 5 shows the cross-sections of various clinched joints. It can be noted that a defect-free clinched joint, which means that the joint is characterized by sufficient interlocking and no neck cracks, can be successfully produced within each type of sheet stack-up. Furthermore, at least one gap can be observed in the joint area between the top sheet and bottom sheet, which is different from the case when the top and bottom sheets have the same sheet thickness as that shown in Ref. [33]. The gap may be generated due to the poorly coordinated deformation capacity of sheet material in the novel dieless clinching process when the two sheets to be joined have diverse sheet thicknesses.

To better reveal the effect of sheet thickness ratio on the neck thickness and interlock width of the novel dieless clinched joints, a qualitative and quantitive analysis regarding the neck thickness and interlock width of various clinched joints was carried out.

Figure 6 demonstrates the effect of sheet thickness ratio on the neck thickness of the novel dieless clinched joints. As can be noted, with the sheet thickness ratio increasing, the joint neck thickness exhibits a trend of continuous growth. In the case of the minimum sheet thickness ratio of 0.5 (1.5-3 joint), the joints neck thickness is 0.15 mm. However, in the case of the maximum sheet thickness ratio of 2.0 (3-1.5 joint), the joint neck thickness is 0.59 mm, which is almost 3 times larger than the joint neck thickness with the minimum sheet thickness ratio.

Figure 7 demonstrates the effect of sheet thickness ratio on the interlock width of the novel dieless clinched joint. Different from the case of neck thickness, the joint interlock width tends to increase first and then decline with the sheet thickness ratio growing. Among these joints, the joint with the thickness ratio of 0.8 (2-2.5 joint) has the maximum interlock width (0.35 mm), while the joint with the thickness ratio of 2.0 (3-1.5 joint) has the minimum interlock width (0.12 mm).

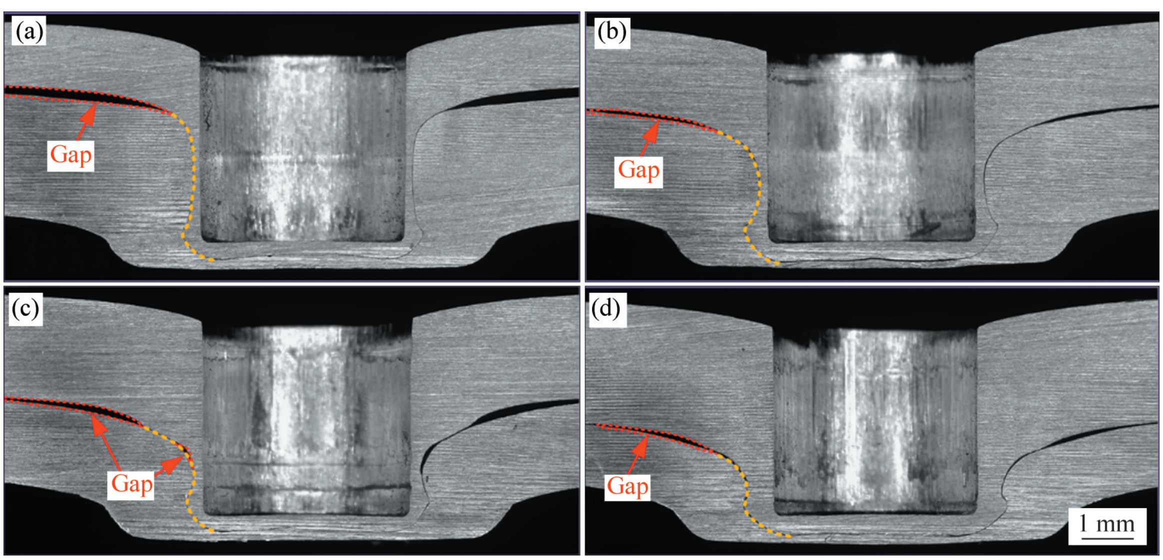

Figure 5 Cross-sections of various clinched joints: (a) 1.5-3 joint; (b) 2-2.5 joint; (c) 2.5-2 joint; and (d) 3-1.5 joint

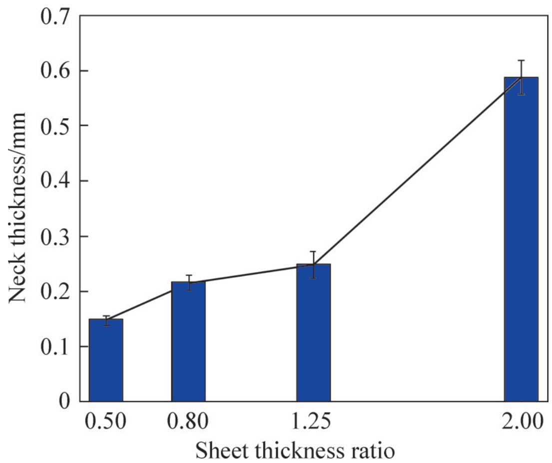

Figure 6 Effect of sheet thickness ratio on the neck thickness of the novel dieless clinched joint

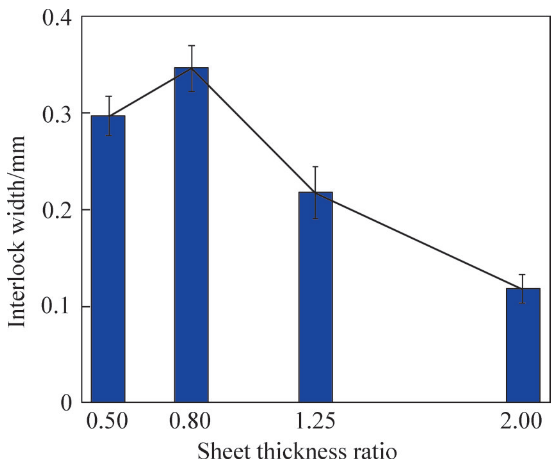

Figure 7 Effect of sheet thickness ratio on the interlock width of the novel dieless clinched joint

3.2 Microhardness analysis

Due to the heterogeneity of the sheet metal plastic deformation behavior during the clinching process, the work-hardening behavior of the clinched sheets varies depending on the region of clinched joint [42]. The hardness distribution of joint cross-sections can reflect the work-hardening and thus the plastic deformation is suffered by the sheets to some extent. Hence, in order to have an in-depth understanding of the sheet plastic deformation behavior in the dieless clinching process, the microhardness distributions of joints with different sheet thickness ratios were contrastively analyzed. Figure 8 illustrates the microhardness distribution of 1.5-3 joint and 3-1.5 joint. The microhardness of the base material is approximately $HV_{0.05}$ 90. As can be noted, regardless of the sheet stacking sequence (small or large sheet thickness ratio), the maximum microhardness occurred in the neck area of the top sheet. The microhardness of the top sheet material adjacent to the corner and bottom of the punch is approximately close and ranks only second to that of the top sheet neck. Furthermore, the top sheet microhardness is significantly greater than the bottom sheet microhardness, which means that the top sheet material underwent a severer plastic deformation than the bottom sheet in the novel dieless clinching process.

By comparing the microhardness distribution of 1.5-3 joint and 3-1.5 joint, it is shown that the top sheet microhardness of 1.5-3 joint is much greater than that of 3-1.5 joint, which indicates that a relatively thin top sheet may suffer greater plastic deformation in the novel dieless clinching process.

3.3 Failure behavior

To study the failure behavior of the novel dieless clinched joints with various sheet thickness ratios, both the load−displacement curves and joint cross-sections after failure were analyzed.

Figure 9 shows the typical tensile-shear load−displacement curves and joint cross-sections after failure. As can be noted, the tensile-shear load−displacement curves of various joints exhibit a

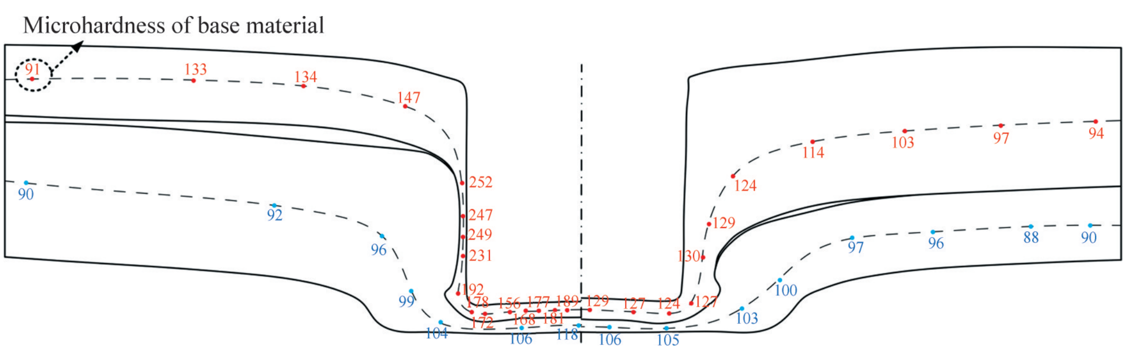

Figure 8 The $HV_{0.05}$ microhardness distribution of 1.5-3 joint (left) and 3-1.5 joint (right)

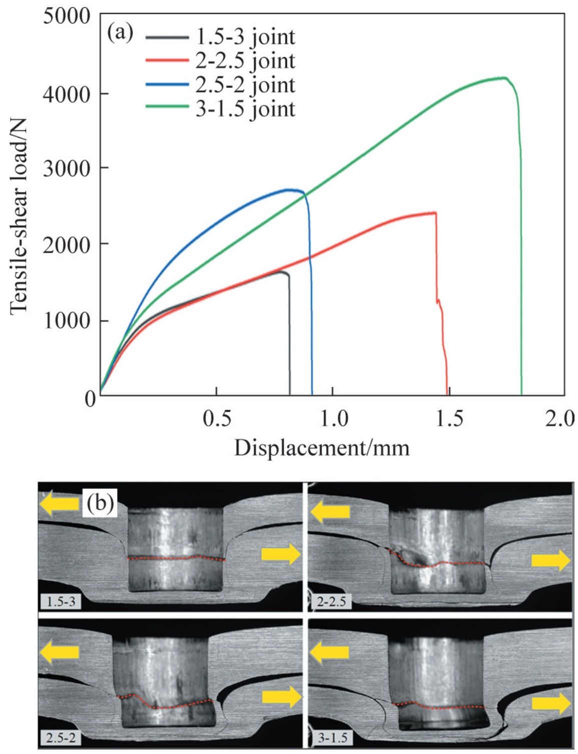

Figure 9 Typical tensile-shear load−displacement curves (a) and joint cross-sections after failure (b)

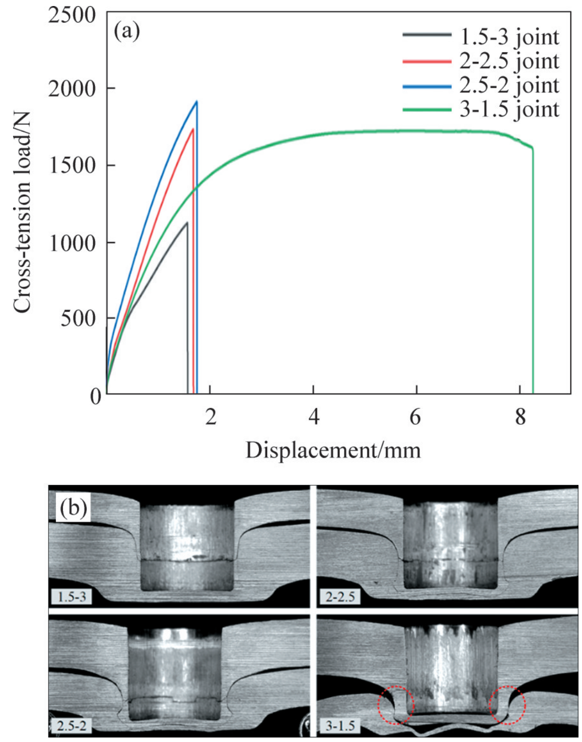

Figure 10 Typical cross-tension load − displacement curves (a) and joint cross-sections after failure (b)

similar trend. Among these curves, the 3-1.5 joint curve has the maximal load and displacement, while the 1.5-3 joint curve has the minimal load and displacement.

From the joint cross-sections after failure shown in Figure 9(b), it can be noted that all joints failed due to neck fracturing. However, some difference can be found regarding the fractured line (red dashed line in Figure 9(b)) between the 1.5-3 joint and the other three joints. From the cross-sectional perspective, the fractured line of the 1.5-3 joint is almost straight while the fractured lines of 2-2.5, 2.5-2 and 3-1.5 joints are broken lines with steps. By comparing the joint cross-sections before (shown in Figure 5) and after failure, it can be inferred that during the tensile-shear test, the 2-2.5, 2.5-2 and 3-1.5 joints underwent significant plastic deformation before failure while hardly any plastic deformation signal can be found in 1.5-3 joint.

Figure 10 shows the typical cross-tension load−displacement curves and joint cross-sections after failure. It can be seen from Figure 10(a) that the cross-tension load − displacement curves of 1.5-3, 2-2.5 and 2.5-2 joints are different from that of 3-1.5 joint. A very slow and persistent growing stage can be found in the 3-1.5 joint curve, resulting in its large displacement.

Furthermore, two different failure modes can be found in these joints. The 1.5-3, 2-2.5 and 2.5-2 joints exhibit a failure mode of neck fracture while the 3-1.5 joint exhibits a failure mode of button separation. Besides, due to the severe bending deformation occurring in the bottom sheet of the 3-1.5 joint, the axial force suffered by the joint may become asymmetrical, which sped up the button separation process.

3.4 Mechanical properties

3.4.1 Strength

Figure 11 shows the effect of sheet thickness ratio on the tensile-shear strength of the novel dieless clinched joint. As can be noted, with the sheet thickness ratio increasing, the tensile-shear strength tends to increase continuously. When the sheet thickness ratio is 2.0 (3-1.5 joint), the tensile-shear strength reaches its maximum, i. e. 3996.2 N, which is nearly 140% higher than the case when the sheet thickness ratio is 0.5 (1.5-3 joint). In addition, it can be found that the tensile-shear strengths of 2-2.5 joint (sheet thickness ratio of 0.8) and 2.5-2

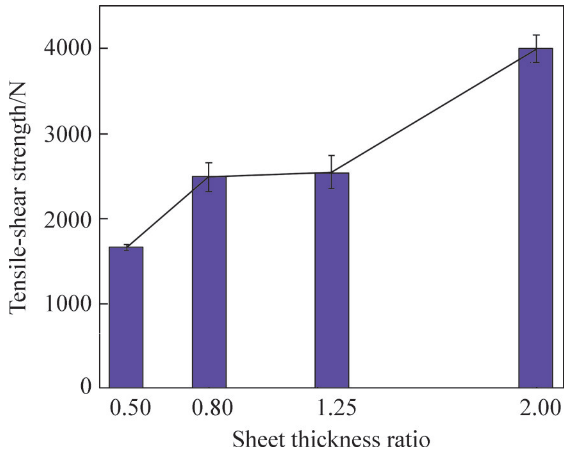

Figure 11 Effect of sheet thickness ratio on the tensile-shear strength of the novel dieless clinched joint

(sheet thickness ratio of 1.25) joint are very close, which indicates that the sheet stacking sequence has a limited effect on the joint shear strength when the sheet thickness is close.

During the tensile-shear test, the thinnest region of the top sheet, i.e. the joint neck, is easy to be fractured under shear load. Hence, the tensile-shear strength of clinched joint highly depends on the neck thickness. As can be noted from Figure 6, with the sheet thickness ratio increasing, the joint neck thickness grows continually, which leads to the continuously growing trend of joint tensile-shear strength.

Figure 12 shows the effect of sheet thickness ratio on the cross-tension strength of the novel dieless clinched joint. With the sheet thickness ratio increasing, the cross-tension strength of the novel dieless clinched joint exhibits a tendency to increase and then decrease. When the sheet thickness ratio is

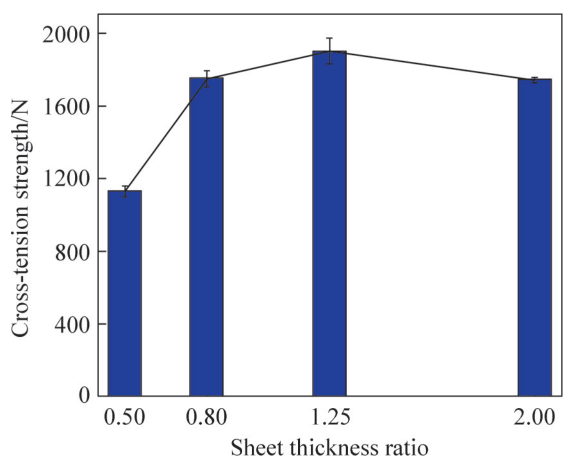

Figure 12 Effect of sheet thickness ratio on the cross-tension strength of the novel dieless clinched joint

1.25 (2.5-2 joint), the cross-tension strength reaches its maximum of 1902 N. Furthermore, when the thicknesses of the sheets to be connected are 1.5 mm and 3 mm, the cross-tension strength of 1.5-3 joint (sheet thickness ratio of 0.5) is 1130 N, while the cross-tension strength of 3-1.5 joint (sheet thickness ratio of 2.0) is 1742 N. The cross-tension strength of 3-1.5 joint is 54% higher than that of 1.5-3 joint, which indicates that the sheet stacking sequence has a crucial effect on the cross-tension strength of the novel dieless clinched joint, especially when significant sheet thickness difference exists between both sheets.

During the cross-tension test, both the interlock and neck of clinched joint suffered plastic deformation under axial load. The clinched joint failed when the inlaid top sheet material was completely removed from the interlocking structure (i.e. failure by button separation), or when the neck was thinned and even fractured (i.e. failure by neck fracture). Therefore, the cross-tension strength of the clinched joint is determined by both the interlock width and neck thickness. And when the joint failed due to neck fracture, the cross-tension strength mainly depended on neck thickness. When the joint failed due to button separation, the cross-tension strength mainly depended on interlock width. Hence, the initial growth of the joint cross-tension strength is caused by the increasing neck thickness (see Figure 6) while the late decline of the joint cross-tension strength can be attributed to the weakened interlock width (see Figure 7).

3.4.2 Absorbed energy

In the case of collision, the vehicle structure with higher impact resistance and energy absorption ability can ensure the safety of passengers more effectively. To this end, the effect of sheet thickness ratio on the absorbed energy of the novel dieless clinched joint in the tensile-shear test is investigated. As can be noted from Figure 13, energy absorbed by the joint is characterized by an overall trend of growth with the sheet thickness ratio increasing. In the case of a sheet thickness ratio of 0.5, the joint energy absorption is 1.1 J, while in the case of a sheet thickness ratio of 2.0, the joint energy absorption is up to 4.6 J (about 3.2 times more than the case of sheet thickness ratio of 0.5). Furthermore, the absorbed energy of 2.5-2 joint (sheet thickness ratio of 1.25) is slightly less than that of 2-2.5 joint (sheet thickness ratio of 0.8),

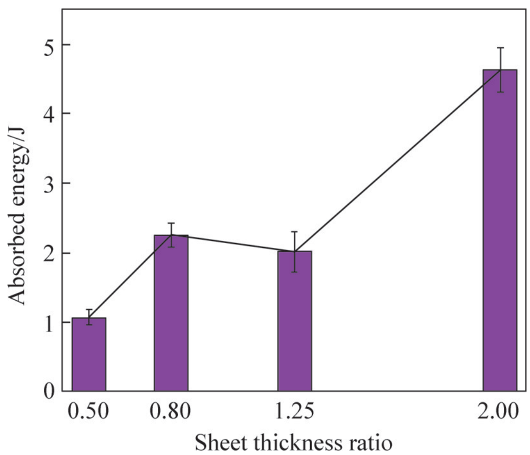

Figure 13 Effect of sheet thickness ratio on the absorbed energy of the novel dieless clinched joint

which can be attributed to the relatively smal displacement of 2.5-2 joint in tensile-shear test (see Figure 9).

3.4.3 Instantaneous stiffness

The instantaneous stiffness of the clinched joint, which can be calculated by the ratio of strength to displacement, was also investigated in this study. Figure 14 shows the instantaneous stiffness−displacement curves of various joints in the tensile-shear test. As can be noted, for all joints, the instantaneous stiffness decreased gradually with the increase of displacement. Furthermore, the instantaneous stiffness−displacement curve can be divided into three stages according to the slope. In the first stage and third stage, the joint stiffness decreases rapidly while in the second stage, a relatively gradual change regarding the joint stiffness can be observed. There exists a visible

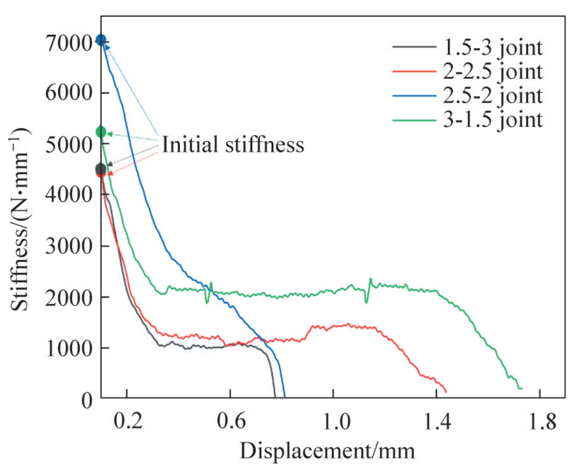

Figure 14 Instantaneous stiffness−displacement curves of various joints in tensile-shear test

difference regarding the stiffness−displacement curves of joints with various sheet thickness ratios. Among these joints, the 2.5-2 joint exhibits the highest initial stiffness while the 1.5-3 joint and 2-2.5 joint exhibit comparatively lower initial stiffness, which indicate that the 2.5-2 joint has the highest non-deformability under shear load.

4 Conclusions

In this research, the novel dieless clinching process was implemented to join AA6061 sheets with thicknesses of 1.5, 2.0, 2.5 and 3.0 mm according to four different sheet stack-ups. The effects of the sheet thickness ratio on the joint failure behavior and mechanical properties were revealed experimentally. From the results, the main conclusions can be drawn:

1) The AA6061 sheets with thicknesses of 1.5 mm, 2.0 mm, 2.5 mm and 3.0 mm can be successfully joined by the novel dieless clinching process whatever the sheet stack-up is.

2) The joints with different sheet thickness ratios exhibit different failure behavior. In the tensile-shear test, the 2-2.5, 2.5-2 and 3-1.5 joints suffered significant plastic deformation before neck fracture while the 1.5-3 joint suffered inappreciable plastic deformation before neck fracture. In the cross-tension test, the 1.5-3, 2-2.5 and 2.5-2 joints failed due to neck fracture while 3-1.5 joint failed due to button separation.

3) Sheet thickness ratio influences the mechanical properties of the joint. With the increase of sheet thickness ratio, the tensile-shear strength is enhanced, the cross-tension strength is enhanced firstly and then reduced and the absorbed energy exhibits an overall trend of growth.

4) In general, it is more appropriate to employ a relatively thick sheet for the top sheet (i.e. large sheet thickness ratio) in the novel dieless clinching process to ensure better joint performance.

Contributors

QIN Deng-lin performed the experiments, analyzed the measured data and wrote the original draft; CHEN Chao provided the concept and methodology. All authors replied to reviewers' comments and revised the final version.

Conflict of interest

QIN Deng-lin and CHEN Chao declare that they have no conflict of interest.

References

[1] OU He-guo, TANG Xiao-dong, XIAO Jie-ping, et al. Lightweight body-in-white design driven by optimization technology [J]. Automotive Innovation, 2018, 1(3): 255−262. DOI: 10.1007/s42154-018-0032-x.

[2] REN Xiao-qiang, CHEN Chao, RAN Xiang-kun, et al. Microstructure evolution of AA5052 joint failure process and mechanical performance after reconditioning with tubular rivet [J]. Transactions of Nonferrous Metals Society of China, 2021, 31(11): 3380−3393. DOI: 10.1016/S1003-6326(21)65736-9.

[3] LI Ming-feng, WANG Yan-jun, NIU Zhen, et al. Study on the weld-bonding process optimization and mechanical performance of aluminum alloy joints [J]. Automotive Innovation, 2020, 3(3): 221−230. DOI: 10.1007/s42154-020-00106-0.

[4] ZHAO Huan, HAN Li, LIU Yun-peng, et al. Analysis of joint formation mechanisms for self-piercing riveting (SPR) process with varying joining parameters [J]. Journal of Manufacturing Processes, 2022, 73: 668−685. DOI: 10.1016/j.jmapro.2021.11.038.

[5] LI Ze-cheng, DENG Yun-lai, YUAN Man-fa, et al. Effect of isothermal compression and subsequent heat treatment on grain structures evolution of Al-Mg-Si alloy [J]. Journal of Central South University, 2021, 28(9): 2670−2686. DOI: 10.1007/s11771-021-4801-z.

[6] ZHANG Jin-liang, YE Jie-liang, SONG Bo, et al. Comparative study on microstructure and electrochemical corrosion resistance of Al7075 alloy prepared by laser additive manufacturing and forging technology [J]. Journal of Central South University, 2021, 28(4): 1058−1067. DOI: 10.1007/s11771-021-4679-9.

[7] SABRA A M K, JAIN M K. Die-less clinching process and joint strength of AA7075 aluminum joints [J]. Thin-Walled Structures, 2017, 120: 421−431. DOI: 10.1016/j.tws.2017.06.021.

[8] MORI K I, ABE Y. A review on mechanical joining of aluminium and high strength steel sheets by plastic deformation [J]. International Journal of Lightweight Materials and Manufacture, 2018, 1(1): 1−11. DOI: 10.1016/j.ijlmm.2018.02.002.

[9] MORI K I, BAY N, FRATINI L, et al. Joining by plastic deformation [J]. CIRP Annals, 2013, 62(2): 673−694. DOI: 10.1016/j.cirp.2013.05.004.

[10] ALVES L M, AFONSO R M, SILVA F L R, et al. Deformation-assisted joining of sheets to tubes by annular sheet squeezing [J]. Materials (Basel, Switzerland), 2019, 12(23): 3909. DOI: 10.3390/ma12233909.

[11] LI De-zhi, CHRYSANTHOU A, PATEL I, et al. Self-piercing riveting-a review [J]. The International Journal of Advanced Manufacturing Technology, 2017, 92(5−8): 1777−1824. DOI: 10.1007/s00170-017-0156-x.

[12] ZIRNGIBL C, DWORSCHAK F, SCHLEICH B, et al. Application of reinforcement learning for the optimization of clinch joint characteristics [J]. Production Engineering, 2022, 16(2−3): 315−325. DOI: 10.1007/s11740-021-01098-4.

[13] LAMBIASE F, KO D C. Two-steps clinching of aluminum and carbon fiber reinforced polymer sheets [J]. Composite Structures, 2017, 164: 180−188. DOI: 10.1016/j.compstruct.2016.12.072.

[14] MUCHA J. The numerical analysis of the effect of the joining process parameters on self-piercing riveting using the solid rivet [J]. Archives of Civil and Mechanical Engineering, 2014, 14(3): 444−454. DOI: 10.1016/j.acme.2013.11.002.

[15] DAS A, LI De-zhi, WILLIAMS D, et al. Joining technologies for automotive battery systems manufacturing [J]. World Electric Vehicle Journal, 2018, 9(2): 22. DOI: 10.3390/wevj9020022.

[16] ABE Y, ISHIHATA S, MAEDA T, et al. Mechanical clinching process using preforming of lower sheet for improvement of joinability [J]. Procedia Manufacturing, 2018, 15: 1360−1367. DOI: 10.1016/j.promfg.2018.07.347.

[17] ABE Y, SAITO T, MORI K I, et al. Mechanical clinching with dies for control of metal flow of ultra-high-strength steel and high-strength steel sheets [J]. Proceedings of the Institution of Mechanical Engineers, Part B: Journal of Engineering Manufacture, 2018, 232(4): 644−649. DOI: 10.1177/0954405416683429.

[18] ESHTAYEH M, HRAIRI M. Multi objective optimization of clinching joints quality using Grey-based Taguchi method [J]. The International Journal of Advanced Manufacturing Technology, 2016, 87(1−4): 233−249. DOI: 10.1007/s00170-016-8471-1.

[19] LAMBIASE F, ILIO A D. Optimization of the clinching tools by means of integrated FE modeling and artificial intelligence techniques [J]. Procedia CIRP, 2013, 12: 163−168. DOI: 10.1016/j.procir.2013.09.029.

[20] WANG Xiao, LI Xin-ding, SHEN Zong-bao, et al. Finite element simulation on investigations, modeling, and multiobjective optimization for clinch joining process design accounting for process parameters and design constraints [J]. The International Journal of Advanced Manufacturing Technology, 2018, 96(9−12): 3481−3501. DOI: 10.1007/s00170-018-1708-4.

[21] WANG Meng-han, XIAO Gui-qian, LI Zhi, et al. Shape optimization methodology of clinching tools based on Bezier curve [J]. The International Journal of Advanced Manufacturing Technology, 2018, 94(5−8): 2267−2280. DOI: 10.1007/s00170-017-0987-5.

[22] SCHWARZ C, KROPP T, KRAUS C, et al. Optimization of thick sheet clinching tools using principal component analysis [J]. The International Journal of Advanced Manufacturing Technology, 2020, 106(1−2): 471−479. DOI: 10.1007/s00170-019-04512-5.

[23] PENG Hao, CHEN Chao, REN Xiao-qiang, et al. Research on the material flow and joining performance of two-strokes flattening clinched joint [J]. Thin-Walled Structures, 2021, 169: 108289. DOI: 10.1016/j.tws.2021.108289.

[24] MUCHA J, KAŠČÁK Ľ, WITKOWSKI W. Research on the influence of the AW 5754 aluminum alloy state condition and sheet arrangements with AW 6082 aluminum alloy on the forming process and strength of the ClinchRivet joints [J]. Materials (Basel, Switzerland), 2021, 14(11): 2980. DOI:

10.3390/ma14112980.
[25] MUCHA J, WITKOWSKI W. The clinching joints strength analysis in the aspects of changes in the forming technology and load conditions [J]. Thin-Walled Structures, 2014, 82: 55−66. DOI: 10.1016/j.tws.2014.04.001.
[26] SALAMATI M, SOLTANPOUR M, ZAJKANI A, et al. Improvement in joint strength and material joinability in clinched joints by electromagnetically assisted clinching [J]. Journal of Manufacturing Processes, 2019, 41: 252−266. DOI: 10.1016/j.jmapro.2019.04.003.
[27] LIN P C, LO S M, WU S P. Fatigue life estimations of alclad AA2024-T3 friction stir clinch joints [J]. International Journal of Fatigue, 2018, 107: 13−26. DOI: 10.1016/j.ijfatigue.2017.10.011.
[28] CHEN Li-wei, CAI M J. Development of a hot stamping clinching tool [J]. Journal of Manufacturing Processes, 2018, 34: 650−658. DOI: 10.1016/j.jmapro.2018.06.022.
[29] ZHANG Yu, ZHANG Xu, GUO Jing, et al. Effects of local stiffness on the spot joints mechanical properties: Comparative study between resistance spot welding and resistance spot clinching joints [J]. Journal of Manufacturing Processes, 2019, 39: 93−101. DOI: 10.1016/j.jmapro.2019.02.018.
[30] WEN Tong, WANG Hui, YANG Chen, et al. On a reshaping method of clinched joints to reduce the protrusion height [J]. The International Journal of Advanced Manufacturing Technology, 2014, 71(9−12): 1709−1715. DOI: 10.1007/s00170-014-5612-2.
[31] NEUGEBAUER R, TODTERMUSCHKE M, MAUERMANN R, et al. Overview on the state of development and the application potential of dieless mechanical joining processes [J]. Archives of Civil and Mechanical Engineering, 2008, 8(4): 51−60. DOI: 10.1016/S1644-9665(12)60121-6.
[32] CHEN Chao, ZHAO Sheng-dun, HAN Xiao-lan, et al. Experimental investigation on the joining of aluminum alloy sheets using improved clinching process [J]. Materials (Basel, Switzerland), 2017, 10(8): 887. DOI: 10.3390/ma10080887.
[33] QIN Deng-lin, CHEN Chao, ZHANG Hui-yang, et al. Experimental investigation of the novel dieless clinching process free of blank holder [J]. Archives of Civil and Mechanical Engineering, 2021, 22(1): 1−12. DOI: 10.1007/s43452-021-00347-8.
[34] ABE Y, MORI K, KATO T. Joining of high strength steel and aluminium alloy sheets by mechanical clinching with dies for control of metal flow [J]. Journal of Materials Processing Technology, 2012, 212(4): 884−889. DOI: 10.1016/j.jmatprotec.2011.11.015.
[35] LEI Lei, HE Xiao-cong, ZHAO De-suo, et al. Clinch-bonded hybrid joining for similar and dissimilar copper alloy, aluminium alloy and galvanised steel sheets [J]. Thin-Walled Structures, 2018, 131: 393−403. DOI: 10.1016/j.tws.2018.07.017.
[36] LÜDER S, HÄRTEL S, BINOTSCH C, et al. Influence of the moisture content on flat-clinch connection of wood materials and aluminium [J]. Journal of Materials Processing Technology, 2014, 214(10): 2069−2074. DOI: 10.1016/j.jmatprotec.2014.01.010.
[37] LAMBIASE F. Mechanical behaviour of polymer-metal hybrid joints produced by clinching using different tools [J]. Materials & Design, 2015, 87: 606−618. DOI: 10.1016/j.matdes.2015.08.037.
[38] LAMBIASE F, DURANTE M, ILIO A D. Fast joining of aluminum sheets with glass fiber reinforced polymer (GFRP) by mechanical clinching [J]. Journal of Materials Processing Technology, 2016, 236: 241−251. DOI: 10.1016/j.jmatprotec.2016.04.030.
[39] CHEN Chao, ZHANG Hui-yang, REN Xiao-qiang, et al. Investigation of flat-clinching process using various thicknesses aluminum alloy sheets [J]. The International Journal of Advanced Manufacturing Technology, 2021, 114(7−8): 2075−2084. DOI: 10.1007/s00170-021-06981-z.
[40] GAO Xiao-lei, CHEN Chao, REN Xiao-qiang, et al. Investigation on failure mechanism of the square clinched joints with different sheet thicknesses [J]. Engineering Failure Analysis, 2022, 134: 106013. DOI: 10.1016/j.engfailanal.2021.106013.
[41] ZHANG Long, LI Ke, HE Hong, et al. Influence of prolonged natural aging followed by artificial aging on tensile properties and compressive behavior of a thin-walled 6005 aluminum alloy tube [J]. Journal of Central South University, 2021, 28(9): 2647−2659. DOI: 10.1007/s11771-021-4799-2.
[42] KALICH J, FÜSSEL U. Design of clinched joints on the basis of binding mechanisms [J]. Production Engineering, 2022, 16(2−3): 213−222. DOI: 10.1007/s11740-022-01108-z.

(Edited by ZHENG Yu-tong)

中文导读

不同板厚比对新型无模压力连接接头的失效行为和力学性能的影响

摘要：作为一种先进且高效的连接方法，压力连接工艺可以实现不同材料或不同厚度板材的连接。本文提出了一种改进的压力连接工艺，即新型无模压力连接工艺，并利用该工艺开展了 1.5 mm、2.0 mm、2.5 mm 和 3.0 mm 四种厚度的 AA6061 铝合金板材的连接实验，研究了接头的几何特征、显微硬度分布、失效行为、静态强度、能量吸收以及瞬时刚度。结果表明，板厚比对新型无模压力连接接头的失效行为和力学性能有显著影响，较大的板厚比有助于提升接头性能。

关键词：连接工艺；压力连接；板厚比；失效行为；力学性能